AIAA Journal
Vol. 45, No. 1, January 2007

Technical Notes

TECHNICAL NOTES are short manuscripts describing new developments or important results of a preliminary nature. These Notes should not exceed 2500 words (where a figure or table counts as 200 words). Following informal review by the Editors, they may be published within a few months of the date of receipt. Style requirements are the same as for regular contributions (see inside back cover).

Bidirectional Evolutionary Topology Optimization for Structures with Geometrical and Material Nonlinearities

X. Huang* and Y. M. Xie†
RMIT University, Melbourne 3001, Australia

DOI: 10.2514/1.25046

I. Introduction

TOPOLOGY optimization methods such as the homogenization method [1,2] and evolutionary structural optimization method [3,4] enable designers to find the best structural layout for required structural performances. So far, most papers dealing with these optimization methods have been concerned with the optimization of structures with linear material and small deformation behavior. However, the linear assumptions are not always valid for applications involving nonlinear material and large deformation. A number of papers have considered topology optimization of geometrically nonlinear structures [5–8]. Topology optimization of materially nonlinear structures has also been conducted by several researchers [9–12]. However, the work on topology optimization with both geometrical and material nonlinearities is limited. Jung and Gea [13] studied topology optimization of both geometrically and materially nonlinear structure using generalized convex approximation (GCA). But their topologies contained gray area (soft material), which leads to difficulties in manufacturing.

The evolutionary structure optimization (ESO) method has been under continuous development since it was first proposed by Xie and Steven [3] in 1993. The ESO method is based on the simple concept of systematically removing inefficient material from the structure after each finite element analysis, so that the resulting design is gradually evolved to an optimum. This method has been extended to a wide range of structural optimization problems [14,15]. To avoid the deficiency of the ESO method, the bidirectional evolutionary structural optimization (BESO) method, which allows the material removed and added to the structure, has been proposed [16,17]. The BESO method provides a more robust and, often, more efficient algorithm for searching for the optimal solution. This is particularly advantageous for problems in which the analysis comprises a large portion of the computational overhead of the topology optimization (e.g., for nonlinear finite element analysis).

Received 14 May 2006; revision received 9 July 2006; accepted for publication 20 September 2006.

*Australian Postdoctoral Fellow, School of Civil and Chemical Engineering, GPO Box 2476V; huang.xiaodong@rmit.edu.au.

†Professor, School of Civil and Chemical Engineering, GPO Box 2476V; mike.xie@rmit.edu.au.

In this paper, the BESO method is applied to the topology optimization for maximizing stiffness of nonlinear structures. By removing and adding elements, the performance of structures is gradually improved. The optimization process will be stopped when both the objective volume and the prescribed termination criterion are satisfied.

Several examples are presented to verify the proposed optimization method. Numerical results show that the stiffness of structures optimized using combined geometrically and materially nonlinear modeling is always higher than that using linear analysis. The improvement is especially significant in cases involving buckling effects.

II. Optimization Problem and Sensitivity Number

In many industrial applications, the maximum stiffness of a structure is pursued. One way to achieve that is by minimizing the mean compliance of the structure that is defined with the area below the load-deflection curve and is equal to the external work in quasi-static condition. When a nonlinear structure is subjected to the external force $\{F\}$, the optimization problem for maximizing stiffness can be formulated with the volume constraint, using the element as the design variable:
minimize

$$C = \int_0^T \{F\}^T \{\dot{\boldsymbol{u}}\}\,\mathrm{d}t \tag{1a}$$

subject to

$$g = V^* - \sum_{i=1}^{n} V_i x_i = 0 \tag{1b}$$

$$x_i \in \{0,\ 1\} \tag{1c}$$

where $\{\dot{\boldsymbol{u}}\}$ represents the visual velocity vectors, T is the integration limit that corresponds to the final state, V_i is the volume of an individual element, V^* is the prescribed total structural volume, and the binary design variable x_i declares the absence (0) or presence (1) of an element.

When the ith element is removed from a structure, the overall stiffness of the structure reduces and, correspondingly, the total strain energy increases. In a linear system, the increase of the total strain energy is equal to the elastic strain energy in the ith element. Similarly, the total elastic and plastic strain energy stored in the ith element is a first-order approximation of the variation of the mean compliance for a nonlinear system, as discussed next. (For a detailed sensitivity analysis, see Buhl et. al. [5] and Jung and Gea [13].)

$$\Delta C_i = E_i^e + E_i^p \tag{2}$$

Therefore, the sensitivity number of the ith element can be defined by its strain energy divided by its volume:

$$\alpha_i = \frac{E_i^e + E_i^p}{V_i} \tag{3}$$

Thus, sensitivity numbers for all elements in the present structure are obtained. These sensitivity numbers will be linearly extrapolated to void elements surrounding the structure that may be added. Elements

Fig. 1 Design domain and support conditions for example 1.

in the present structure will be removed if they satisfy Eq. (4a):

$$\alpha_i \leq \alpha_{\mathrm{th}} \tag{4a}$$

Those elements surrounding the present structure will be added if they satisfy Eq. (4b):

$$\alpha_i > \alpha_{\mathrm{th}} \tag{4b}$$

where α_{th} is the threshold of the sensitivity number that is determined by the target material volume in each iteration. For example, if the target volume for the present iteration is 70%, then elements for which the sensitivity numbers are ranked at the top 70% of all elements (including the void ones) will remain solid or be added, and all other elements will be deleted or remain void.

The cycle of finite element analysis and element removal and addition will be repeated until the objective material volume V^* is reached and the termination criterion defined in the later section is satisfied. The total material volume must be decreased gradually by introducing an evolutionary removal volume ratio RV:

$$V_{j+1} = V_j(1 - RV), \qquad j = 0, 1, 2, 3 \ldots \tag{5}$$

RV is a constant that is specified by the user. Once the objective material volume V^* is reached, RV is set to be zero.

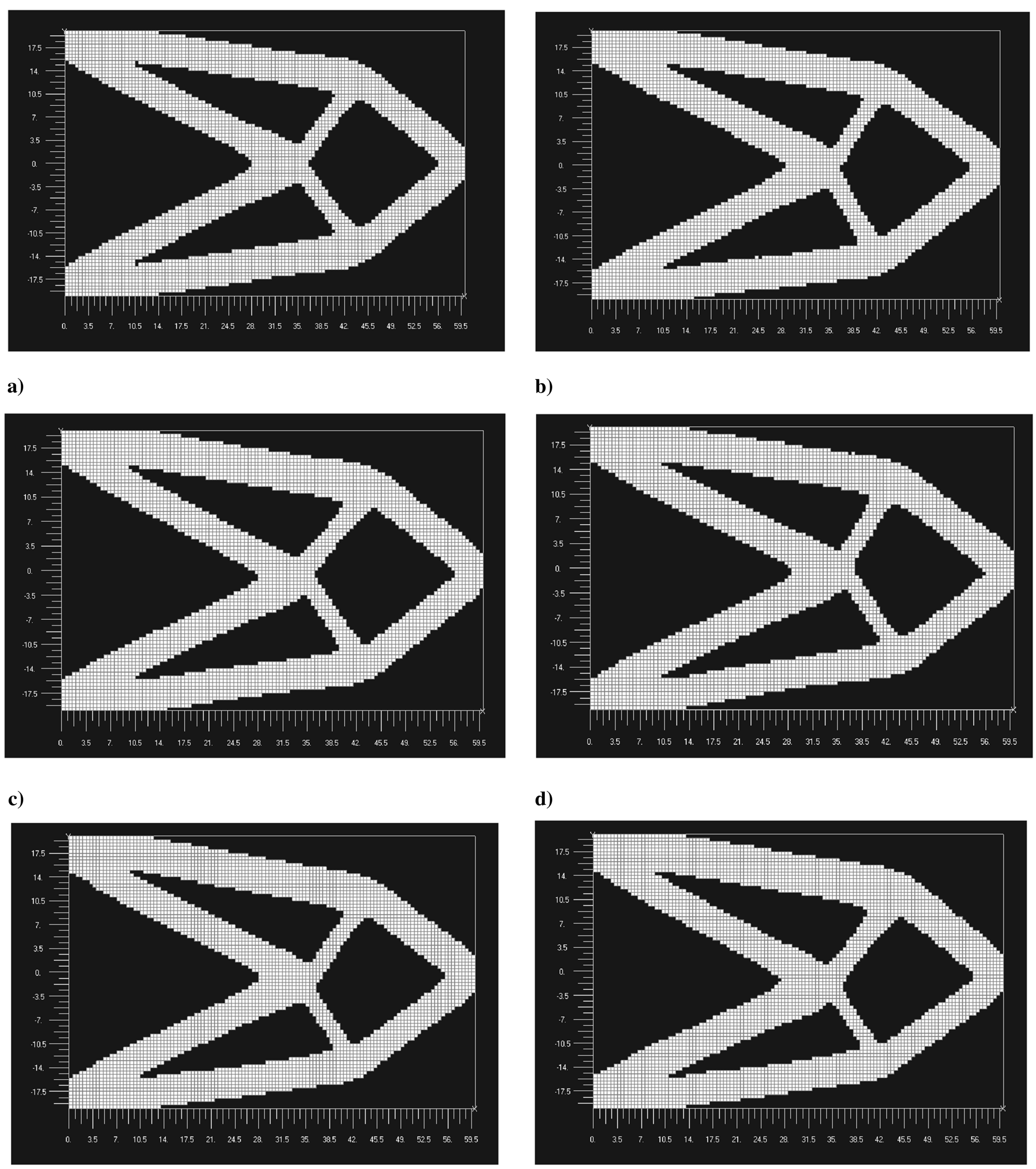

Fig. 2 Optimal topologies with the remaining material ratio $V_f = 40\%$: a) linear optimal design, b) nonlinear optimal design under $P = 400$ N, c) nonlinear optimal design under $P = 600$ N, d) nonlinear optimal design under $P = 800$ N, e) nonlinear optimal design under $P = 1000$ N, and f) nonlinear optimal design under $P = 1100$ N.

Table 1 Comparison of the nonlinear mean compliance between the linear and nonlinear optimums under various loads for example 1

	C, Nmm				
	$P = 400$ N	$P = 600$ N	$P = 800$ N	$P = 1000$ N	$P = 1100$ N
Linear optimum	323.4	735.2	1340.1	2149.9	2638.1
Nonlinear optimum	322.1	729.5	1332.4	2130.3	2515.8

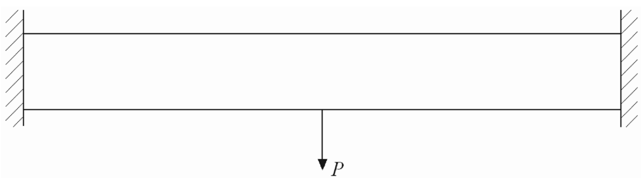

Fig. 3 Design domain and support conditions for example 2.

III. Performance Index and Termination Criterion

In the original BESO method [16,17], the optimization procedure is stopped when the objective material volume is reached. However, that design can be further improved by adjusting the elements and keeping the total material volume constant. Thus, the present BESO procedure continues after the objective material volume is reached and a new termination criterion needs to be defined.

Before we define the termination criterion, a performance index (PI) is first introduced. The performance index is used to identify the efficiency of the optimal designs. In optimization problems for maximizing the stiffness, the stiffness per unit volume denotes the

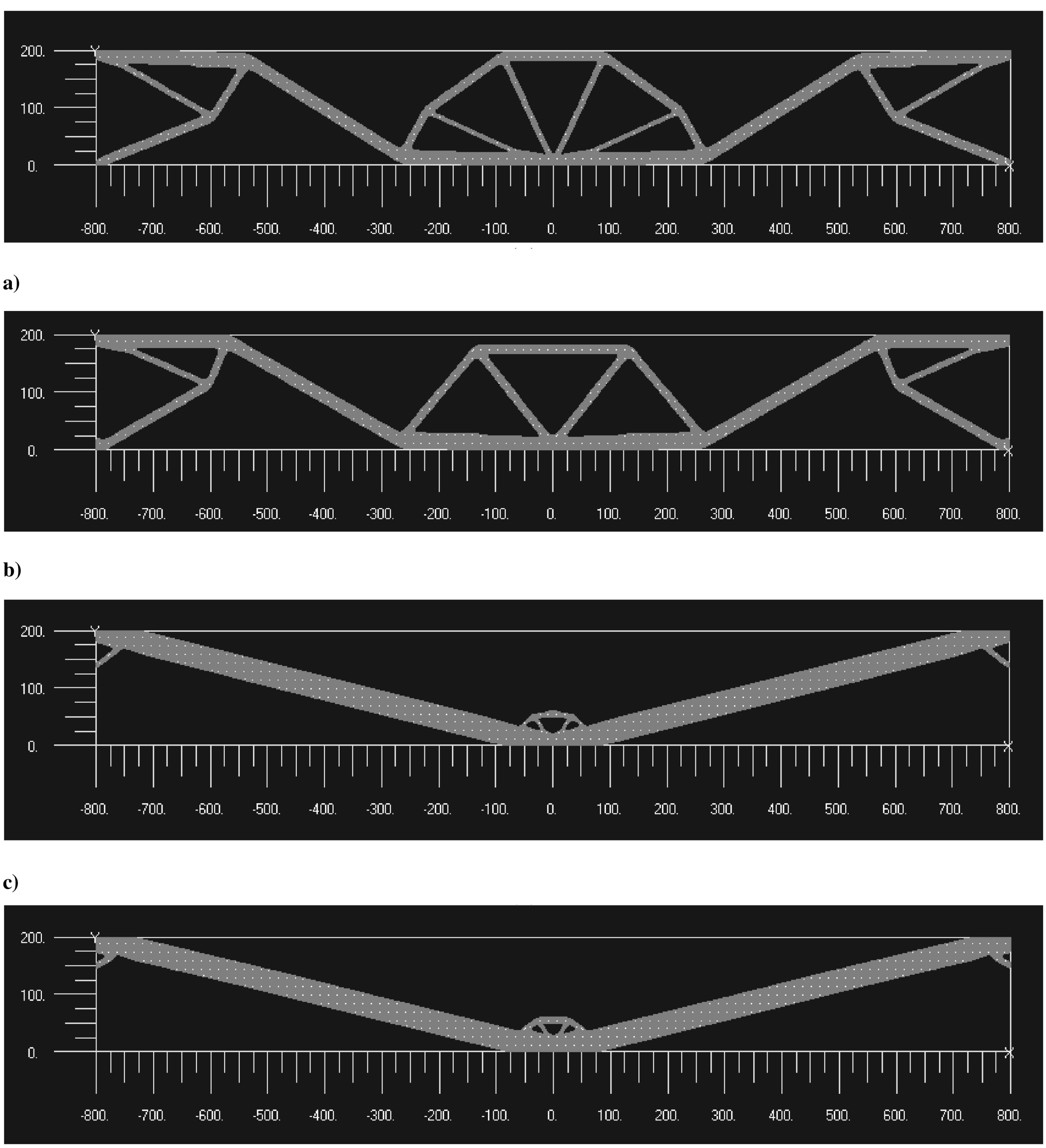

Fig. 4 Optimal topologies using various FE analysis: a) linear, b) materially nonlinear, c) geometrically nonlinear, and d) combined geometrically and materially nonlinear.

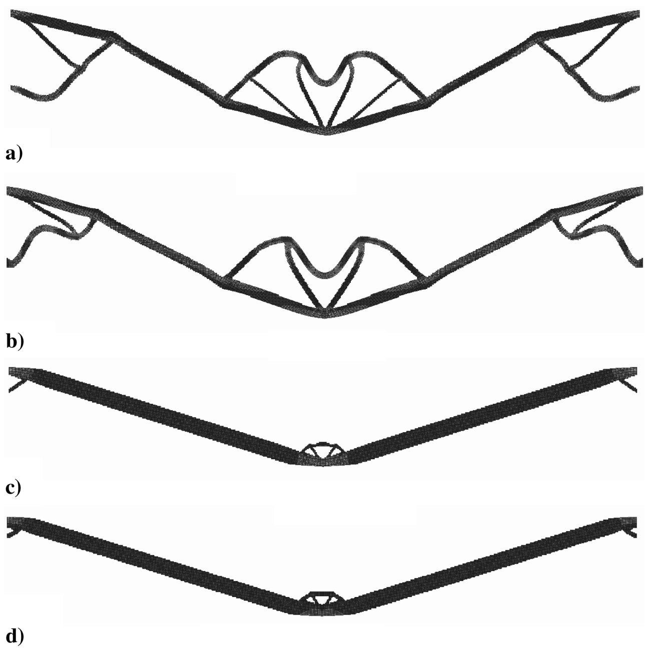

Fig. 5 Deformation of various optimums under the design load: a) linear, b) materially nonlinear, c) geometrically nonlinear, and d) combined geometrically and materially nonlinear.

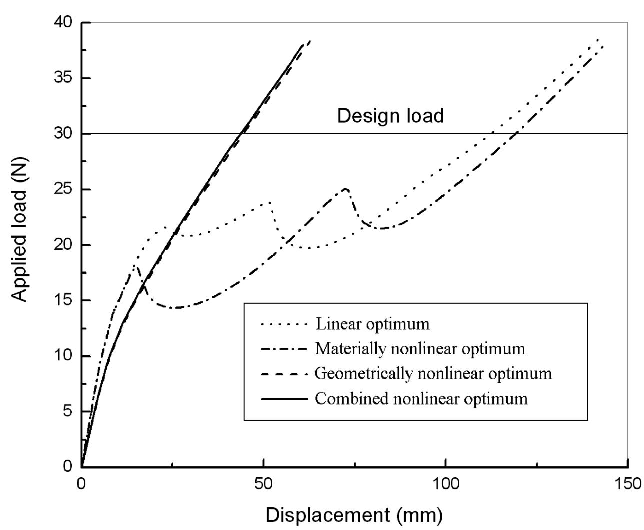

Fig. 6 Comparison of the force-displacement relationships for various optimal designs.

efficiency of the usage of the material and can be therefore be used as a performance index. It is written as

$$PI = 1/CV \tag{6}$$

where C and V are the total mean compliance and the volume of the current design. The design with the highest performance index is the one with the highest stiffness for the same material volume. In the later stage of the present BESO method, the topology of the design continues to adjust by removing and adding elements after the objective volume V^* is reached. Thus, the performance index will be increased step by step. When the performance index of the design has an insignificant improvement over the last design, the optimization process can be stopped. So the performance index of two successive designs is used to define the termination criterion:

$$\text{error}_j = \frac{|PI_j - PI_{j-1}|}{PI_j} \leq \text{error}^* \tag{7}$$

where error_j is the defined performance error for the jth iteration, and error^* is the maximum allowable error that is specified by the user, normally 0.01%.

IV. Examples and Discussion

A. Example 1

To verify the proposed method, the first example studies a cantilever beam with a tip load, shown in Fig. 1. This is a classical problem in the topology optimization of linear structures. We solve this problem considering both geometrical and material nonlinearities. The 60×40 mm design domain (with 10-mm thickness) is meshed using 120×80 4-node quadrilateral elements. The mechanical properties of the assumed bilinear material are Young's modulus $E = 1$ GPa, Poisson's ratio $v = 0.3$, the hardening modulus $E_p = 0.3E$, and yield stress $\sigma_y = 100$ MPa. Five different load magnitudes (400, 600, 800, 1000, and 1100 N) are applied to the middle of the free end. The objective volume is 40% of the design domain. The BESO parameters are $RV = 1\%$ and $error^* = 0.1\%$.

For optimization problems using linear analysis, the optimal topology would not depend on the magnitude of the load. The symmetrical optimum obtained for linear analysis is shown in Fig. 2a. When the combined geometrically and materially nonlinear analyses are used, the resultant topologies are shown in Figs. 2b–2f for the corresponding load magnitudes. The total iterations are 16, 19, 16, 16, and 17, respectively. It can be seen that the nonlinear topology for a small load (e.g., 400 N) is almost the same as the linear topology. The nonlinear topologies become less and less symmetric as the load increases. Table 1 shows the comparison of the nonlinear mean compliance between the linear and nonlinear optimal designs under various loads. We find that the mean compliances for nonlinear optimal design are only marginally lower (i.e., better) than the linear optimal design in this example. However, in some cases, the difference of the mean compliance between the linear and nonlinear optimized structures can be enormous, as will be seen in the next example.

B. Example 2

The design domain of a long, slender beam is shown in Fig. 3. The beam is 1600-mm long, 200-mm deep, and 10-mm thick. The design load $P = 30$ N is applied at the center of the bottom edge. The material is assumed to be an elastoplastic material model with nonlinear strain-hardening, for which the stress–strain relationship after yield is given by $\sigma = 1.34\varepsilon^{0.5}$. The other properties of the material are Young's modulus $E = 30$ MPa, yield stress $\sigma_y = 0.06$ MPa, and Poisson's ratio $v = 0.3$. The target material volume is only 20% of the design domain. The BESO parameters are $RV = 2\%$ and $\text{error}^* = 0.01\%$.

In this example, four different optimization cases are considered and compared: linear, geometry nonlinear only, material nonlinear only, and combined geometry and material nonlinear. The whole model is discretized using 640×80 4-node quadrilateral elements. The resultant topologies are shown in Fig. 4 and the total iterations are 103, 100, 101, and 99, respectively. It can be seen that topologies from the linear and material nonlinear analyses are quite different from the topology from the combined nonlinear analysis. However, topologies from geometry nonlinear and combined nonlinear analyses are similar.

To examine and compare these different topologies, we reanalyze these four final designs using nonlinear finite element analysis, considering both geometrical and material nonlinearities. Figure 5 shows the deformed shape of each design under the design load. It can be seen that the local buckling occurs in designs for the linear and material nonlinear models. These buckling members significantly reduce the load-carrying capability of the structure. Figure 6 shows the force-displacement relationships for these designs. When the applied load is equal to the design load (30 N), the displacement and the mean compliance are 112.32 mm and 2386.1 Nmm for linear optimum, 118.99 mm and 2351.1 Nmm for material nonlinear optimum, 44.41 mm and 781.5 Nmm for geometry nonlinear

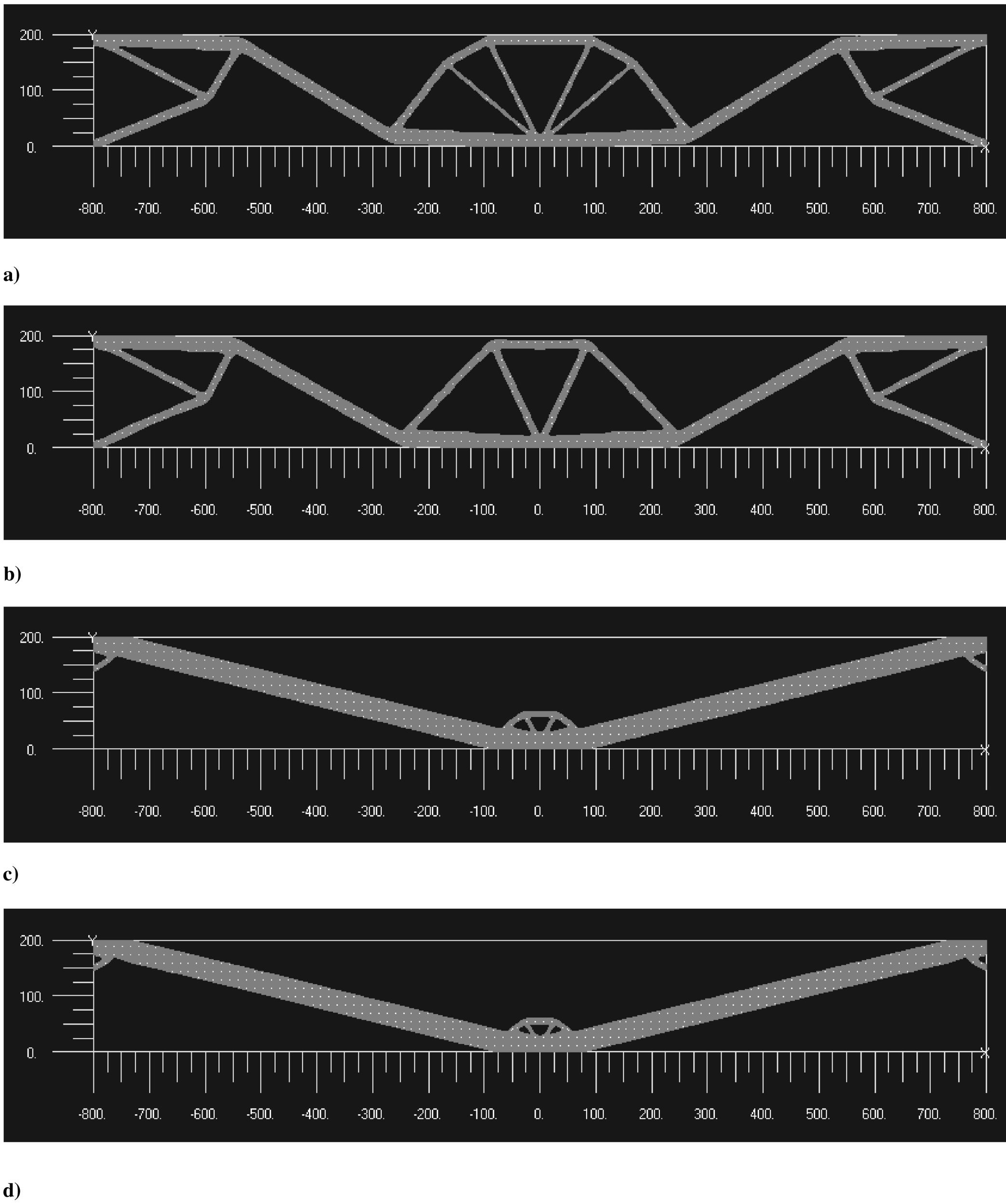

Fig. 7 Optimal topologies under various design loads: a) $P = 10$ N, b) $P = 15$ N, c) $P = 25$ N, and d) $P = 30$ N.

optimum, and 43.65 mm and 770.5 Nmm for combined nonlinear optimum. It can be seen that the combined nonlinear optimum is stiffer than others. Comparing with the linear optimum, the improvement in the stiffness of the combined nonlinear optimum is extremely large.

To investigate the effect of the applied load, the same design problem is considered again, except that we now change the magnitude of the applied load. The optimization is performed with the combined nonlinear analysis. A load of four different magnitudes of load (10, 15, 25, and 30 N) is applied to the middle of the bottom edge. The corresponding optimal topologies are shown in Fig. 7 and the total iterations are 94, 87, 130, and 99, respectively. It is seen that the topology for combined nonlinear analysis and the small load $P = 10$ N is similar to the topology obtained from linear analysis. But when the load increases, the resulting topologies become different as the nonlinear effects become more significant. Detailed comparisons with the mean compliance of linear design are given in Table 2, in which both geometrically and materially nonlinear analyses are applied for all designs.

Table 2 Comparison of the nonlinear mean compliance between the linear and nonlinear optimums under various loads for example 2

	C, Nmm			
	$P = 10$ N	$P = 15$ N	$P = 25$ N	$P = 30$ N
Linear optimum	27.0	78.2	1810.3	2386.1
Nonlinear optimum	26.5	76.8	411.3	770.5

V. Conclusions

In this paper, a topology optimization procedure for the stiffness design of structures with nonlinear material undergoing large, geometrically nonlinear deformations has been proposed by extending the linear bidirectional evolutionary structural optimization (BESO) method. In this procedure, the nonlinear optimization problems are solved through removing and adding elements in the design domain. Thus, the BESO method gains computational efficiency, because the total elements become less and less. Several design problems are investigated to verify the proposed method. Numerical results showed that optimal designs obtained from the combined geometrically and materially nonlinear analyses are always better than optimal designs from linear analysis. The improvement can be very significant for problems involving local buckling.

Acknowledgment

The authors wish to acknowledge the financial support from the Australian Research Council for carrying out this work.

References

[1] Bendsøe, M. P., and Kikuchi, N., "Generating Optimal Topologies in Structural Design Using a Homogenization Method," *Computer Methods in Applied Mechanics and Engineering*, Vol. 71, No. 22, 1988, pp. 197–224.

[2] Bendsøe, M. P., and Sigmund, O., *Topology Optimization: Theory, Methods and Application*, Springer–Verlag, Berlin, 2003.

[3] Xie, Y. M., and Steven, G. P., "A Simple Evolutionary Procedure for Structural Optimization," *Computers and Structures*, Vol. 49, No. 5, 1993, pp. 885–886.

[4] Xie, Y. M., and Steven, G. P., *Evolutionary Structural Optimization*, Springer, London, 1997.

[5] Buhl, T., Pedersen, C. B. W., and Sigmund, O., "Stiffness Design of Geometrically Nonlinear Structures Using Topology Optimization," *Structural and Multidisciplinary Optimization*, Vol. 19, No. 2, 2000, pp. 93–104.

[6] Gea, H. C., and Luo, J., "Topology Optimization of Structures with Geometrical Nonlinearities," *Computers and Structures*, Vol. 79, No. 5, 2001, pp. 1977–1985.

[7] Pedersen, C. B. W., Buhl, T. E., and Sigmund, O., "Topology Synthesis of Large-Displacement Compliant Mechanisms," *International Journal for Numerical Methods in Engineering*, Vol. 50, No. 12, 2001, pp. 2683–2705.

[8] Bruns, T. E., Sigmund, O., and Tortorelli, D. A., "Numerical Methods for the Topology Optimization of Structures that Exhibit Snap-Through," *International Journal for Numerical Methods in Engineering*, Vol. 55, No. 10, 2002, pp. 1215–1237.

[9] Yuge, K., and Kikuchi, N., "Optimization of a Frame Structure Subjected to a Plastic Deformation," *Structural Optimization*, Vol. 10, Nos. 3–4, 1995, pp. 197–208.

[10] Bendsøe, M. P., Guedes, J. M., Plaxton, S., and Taylor, J. E., "Optimization of Structure and Material Properties for Solids Composed of Softening Material," *International Journal of Solids and Structures*, Vol. 33, No. 12, 1996, pp. 1799–1813.

[11] Pedersen, P., "Some General Optimal Design Results Using Anisotropic, Power Law Nonlinear Elasticity," *Structural optimization*, Vol. 15, No. 2, 1998, pp. 73–80.

[12] Mayer, R. R., Kikuchi, N., and Scott, R. A., "Application of Topological Optimization Techniques to Structural Crashworthiness," *International Journal for Numerical Methods in Engineering*, Vol. 39, 1996, pp. 1383–1403.

[13] Jung, D., and Gea, H. C., "Topology Optimization of Nonlinear Structures," *Finite Elements in Analysis and Design*, Vol. 40, No. 11, 2004, pp. 1417–1427.

[14] Chu, D. N., Xie, Y. M., Hira, A., and Steven, G. P., "Evolutionary Structural Optimization for Problems with Stiffness Constraints," *Finite Elements in Analysis and Design*, Vol. 21, No. 4, 1996, pp. 239–251.

[15] Xie, Y. M., and Steven, G. P., "Evolutionary Structural Optimization for Dynamic Problems," *Computers and Structures*, Vol. 58, No. 6, 1996, pp. 1067–1073.

[16] Yang, X. Y., Xie, Y. M., Steven, G. P., and Querin, O. M., "Bidirectional Evolutionary Method for Stiffness Optimization," *AIAA Journal*, Vol. 37, No. 11, 1999, pp. 1483–1488.

[17] Querin, O. M., Young, V., Steven, G. P., and Xie, Y. M., "Computational Efficiency and Validation of Bi-Directional Evolutionary Structural Optimisation," *Computer Methods in Applied Mechanics and Engineering*, Vol. 189, No. 2, 2000, pp. 559–573.

N. Alexandrov
Associate Editor